Journal of Solid State Chemistry **147,** 68–73 (1999)
Article ID jssc.1999.8174, available online at http://www.idealibrary.com on IDEAL®

Correlation Effects in the $NiS_{2-x}Se_x$ System

J. M. Honig

Department of Chemistry, Purdue University, West Lafayette, Indiana 47907-1393

Received October 28, 1998; in revised form January 16, 1999; accepted January 17, 1999

Electrical and selected spectroscopic measurements on single crystal $NiS_{2-x}Se_x$ ($0 \le x \le 0.71$) samples are interpreted in terms of a qualitative band structure scheme that resolves several unusual experimental observations. The guiding principle is that the degree of electron correlation can be controlled by varying the degree of substitution of Se for S. © 1999 Academic Press

INTRODUCTION

There has been recent renewed interest in the electrical properties of the $NiS_{2-x}Se_x$ system because one can drastically alter the degree of electron correlation through substitution of Se for S in the anionic sublattice while keeping the electron concentration constant and the cationic sublattice intact. In contrast, such alterations have generally been achieved in oxides or chalcogenides by aliovalent substitutions in the cation sublattice or by changes in composition, both of which alter the total electron count. Another simplifying aspect is the fact that in first approximation the pyrite structure remains unaltered as the system passes through several transformations. This permits one to concentrate on electronic phenomena without the distracting complications associated with changes in lattice symmetry. However, the electrical properties of $NiS_{2-x}Se_x$ present some puzzles that need to be resolved; this is the subject area of the present paper. Professor Rouxel was greatly interested in the relationship between band structure and electrical characteristics of chalcogenides; thus, it is appropriate to consider certain aspects of the problem in this article which is dedicated to his memory.

The first systematic study of the resistivity and related physical properties of $NiS_{2-x}Se_x$ was published by the DuPont group (1) in the early seventies. Subsequent investigations on both single crystals and polycrystalline specimens are in reasonable accord with this work and with each other. In Fig. 1 we show recent data (2) on the resistivity (ρ) versus temperature (T) of single crystals grown from a Te flux (3); samples obtained by this technique contain no detectable amount of Te. One should note the great variation in electrical characteristics: In the range $0 \le x \lesssim 0.35$ the alloy remains an insulator; plots of $\log \rho$ vs $1/T$ exhibit two regions of linearity, corresponding to conductivity activation energies of 0.33 and 0.11 eV at low and intermediate temperature regions. For compositions $0.38 \lesssim x \lesssim 0.60$ the alloys are metallic-like in the cryogenic temperature range, as judged by the near constancy of the ρ vs T plots. Beyond that point a large rise in ρ with rising T occurs (amounting to factors as large as 700), followed by a maximum, and by an exponential decay of ρ with increasing T; the alloys have transformed into insulators. The compound with $x = 0.38$ exhibits an exceptionally high value of $\rho = 140$ ohm-cm in the *metallic* range below 70 K. Moreover, the sequence of a metal changing to an insulator with increasing temperature is unusual; for most materials undergoing a metal–insulator transition the inverse trend is encountered. For $x \gtrsim 0.60$ the materials are poor metals over the entire measured T range, as signified by a moderate rise of ρ with T. All of these distinctly different characteristics in the same system remain to be explained.

Problems are compounded when one considers the thermoelectric properties of this series; two systematic studies (2, 4) yielded fairly concordant results. Figure 2 shows plots (2) of Seebeck coefficients (α) versus temperature (T). Specimens with low Se content, $0 \le x \lesssim 0.24$, are characterized by small α values in the cryogenic temperature range, precisely where the resistivity is very high. This regime is then followed by a rise of α to large values and by a subsequent decline as T is increased. In contrast, for $x \gtrsim 0.5$ the Seebeck coefficients remain very small and gradually become more negative as T is increased. These trends should also be explained.

We now attempt to address these matters in terms of a proposed band structure that is useful in rationalizing the observations.

QUALITATIVE BAND STRUCTURE SCHEME

We adopted as our point of departure the qualitative band structure scheme originally set up by Goodenough (5) and by Rouxel (6) for chalcogenides. The scheme is based on the hybridization of the Ni e_g and t_{2g} states with the

0022-4596/99 $30.00

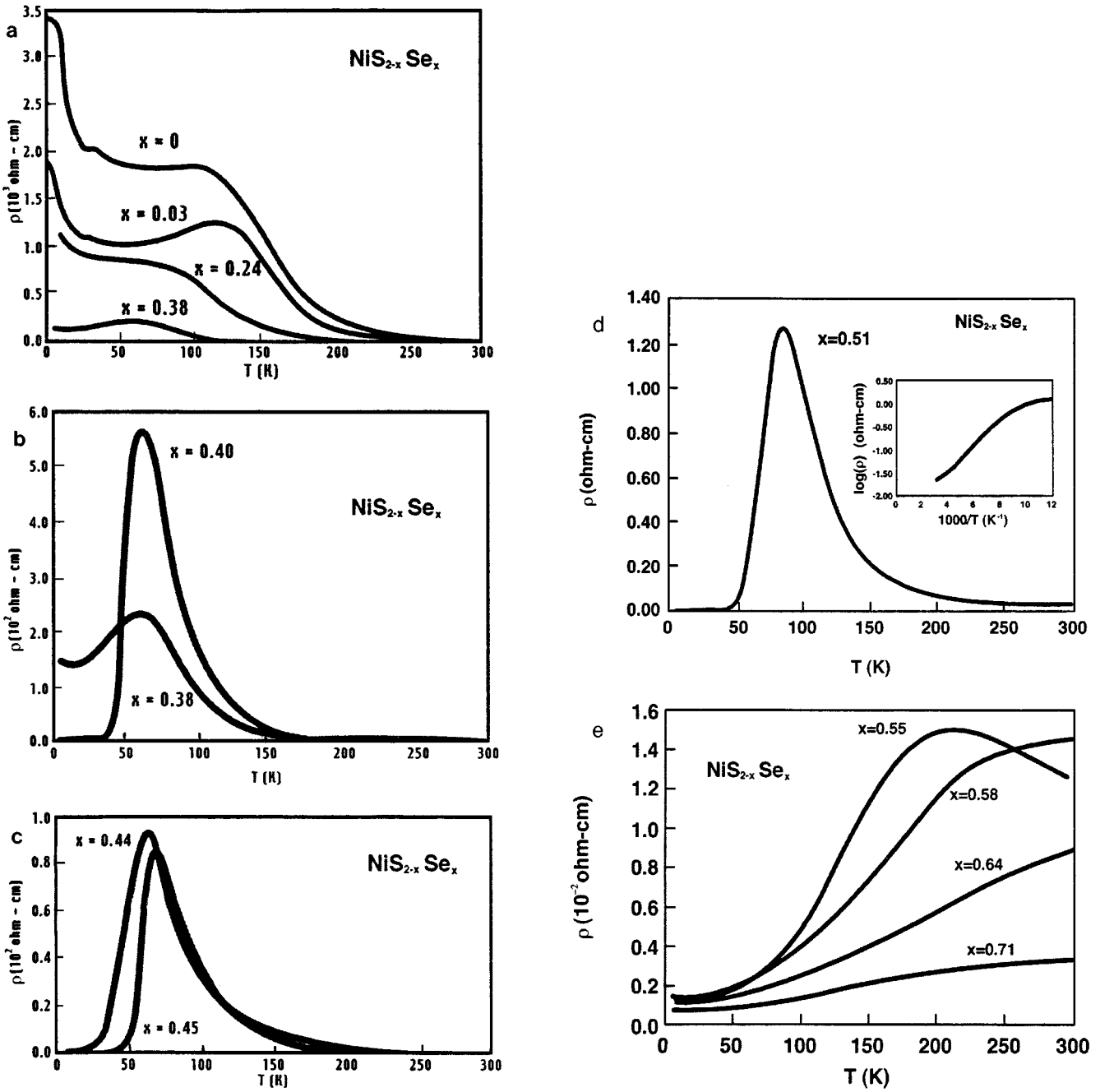

FIG. 1. Resistivity ρ vs temperature T for a variety of $NiS_{2-x}Se_x$ alloys with $0 \leq x \leq 0.71$. Curves line up with the designated compositions. After Ref. (2).

X (X = S, Se) $3p$ or $4p$ states (hereafter designated as $X\ p\sigma$) and with the $(X-X)^{-2}$ molecular units (hereafter designated as $X\ pp\sigma$). Due to symmetry mismatch the t_{2g} linkages are expected to be quite weak, i.e., almost nonbonding. The e_g states hybridize strongly with the anionic states; they therefore lie at the top of the occupied states and broaden into a narrow band through hybridization with the $X\ p\sigma$ orbitals while retaining the e_g type symmetry. The $X\ p\sigma$ states are expected to broaden into a wide band through the same hybridization process. Lastly, the $X\ pp\sigma$ states likely form very narrow bands,through weak e_g hybridization, yielding a bonding and antibonding configuration separated by a large energy gap. The resulting energy band structure is schematically depicted in Fig. 3a. This rather crude presentation is buttressed through more quantitative calculations based on cluster models (7–9).

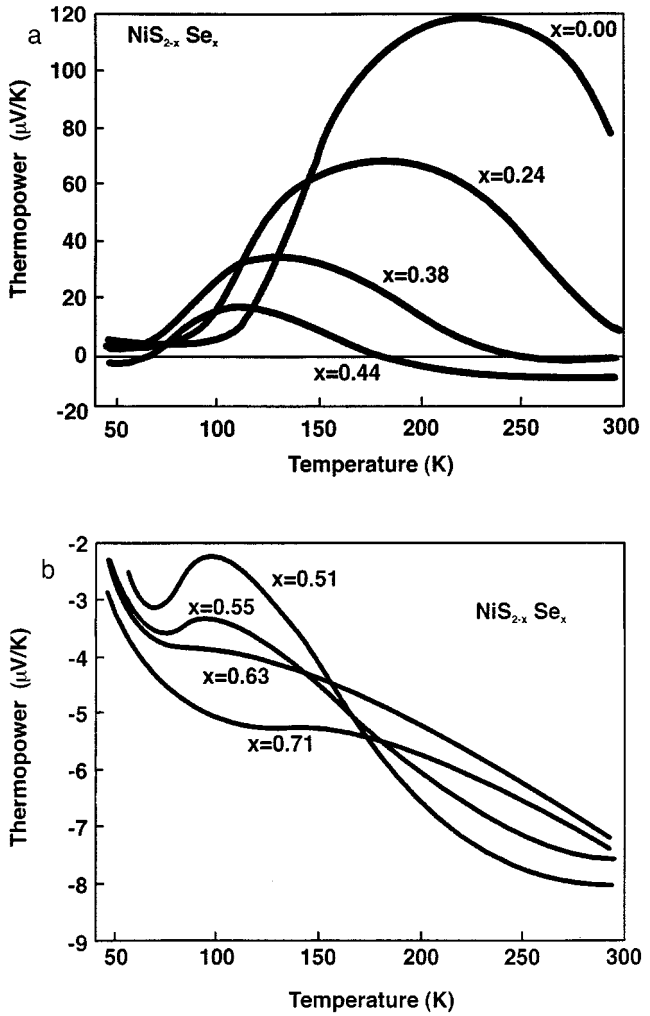

FIG. 2. Seebeck coefficients α vs temperature T for a variety of $NiS_{2-x}Se_x$ alloys with $0 \leq x \leq 0.71$. Curves at 100 K line up with the designated compositions for $x \geq 0.51$.

In stoichiometric $NiS_{2-x}Se_x$ the relatively narrow e_g band is half-filled; the material is then expected to be a poor metal, as is the case for alloys with significant admixture of Se ($x \gtrsim 0.60$). However, as the Se content is reduced one expects the cation–anion orbital overlap to become progressively reduced; correspondingly, the e_g band is narrowed and the electron correlation effects become more significant. Ultimately, a point is reached where the Mott–Hubbard transition sets in: the e_g band is split into two subbands, bonding and antibonding, separated by an energy gap U. This is the situation depicted in Fig. 3b which holds for moderate values of U; at $T = 0$ the lower subband is filled and the upper subband is empty. The material is now an insulator, in consonance with alloys in the range $0 \leq x \lesssim 0.35$. However, an alternative disposition is shown in Fig. 3c; this applies if the gap U is very large. In these circumstances the top of the X $p\sigma^*$ valence band is separated from the bottom of the Ni e_g antibonding band by a gap $\Delta < U$. The material then becomes a charge transfer insulator of the type first described by Zaanen *et al.* (10). Last, we show in Fig. 3d the case where the two gaps are nearly comparable, with Δ only slightly larger than U. Which of these cases applies to the $NiS_{2-x}Se_x$ system must be decided by experiment.

METAL–INSULATOR TRANSITIONS DRIVEN BY ELECTRON CORRELATION EFFECTS

We next show how a metal–insulator transition may be characterized thermodynamically. On a very elementary basis consider first an assembly of N electrons that are frozen on N atomic sites; this represents the limiting case of the half-filled e_g band with zero bandwidth. We take the zero of energy to coincide with the energy of these localized electrons. Their entropy is given by $S_l/N = k_B \ln 2$ (where k_B is the Boltzmann constant), because a given electron can reside on any site in either the *spin up* or the *spin down* configuration with equal probability. The free energy is then given by

$$F_l/N = -k_B T \ln 2. \qquad [1]$$

Next consider an assembly of N itinerant interacting electrons. It may be shown (11) that at low temperatures their heat capacity obeys the Sommerfeld relation $C/N = \gamma T$, but the appropriate Sommerfeld constant γ is related to γ_0 (that of free electrons) through the expression $\gamma = \gamma_0/\Phi$, where Φ is a band narrowing factor $0 \leq \Phi \leq 1$ whose value is specified by the theory (11). For strongly interacting electrons Φ may become quite small, rendering γ very large. This, in fact, is a hallmark of a system of highly correlated charge carriers. The energy of such a collection is specified by $E/N = \int \gamma T dT = \gamma T^2/2 + E_o$ and the entropy is given by $S/N = \int (C/T) dT = \gamma T$. Accordingly, the free energy of the itinerant electrons is

$$F_i/N = E_o - \gamma T^2/2. \qquad [2]$$

We now have a means of ascertaining which state prevails by a comparison of the free energies. In Fig. 4 we show a set of parabolas, representing Eq. [2] for a variety of different intercepts E_o, and a straight line passing through the origin representing Eq. [1]. The value of E_o is dictated by two factors: The first factor is the average kinetic energy of the electron in the e_g band. Relative to the chosen zero of energy this quantity is given by $-\Phi|\bar{\varepsilon}|$, where the band narrowing factor Φ enters again and where $\bar{\varepsilon}$ is the average energy of the equivalent assembly of noninteracting electrons. The second factor is the potential energy of interaction; for simplicity we assume that only two electrons temporarily

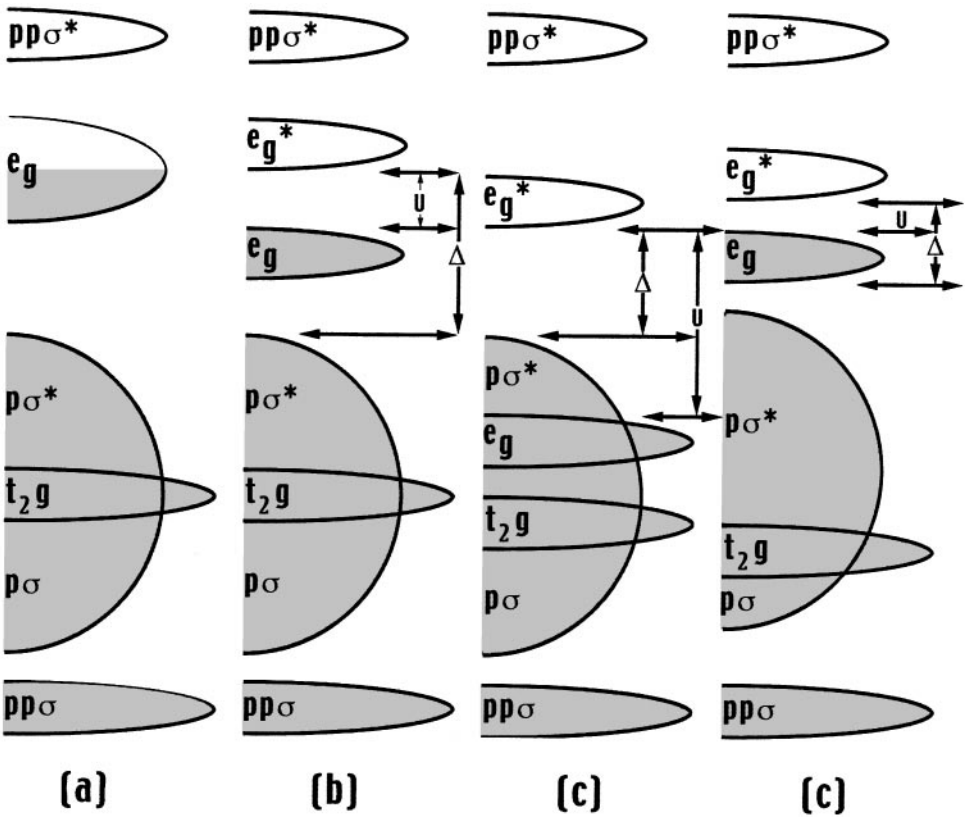

FIG. 3. Proposed qualitative band structure diagram for $NiS_{2-x}Se_x$. Shaded areas indicate occupied band states. For details see text.

residing on the same atomic site interact with a Coulomb repulsion energy U_o. The total repulsion energy is then given by $U_o\eta$, where η is the probability that a given site is doubly occupied by two electrons with reversed spins. Accordingly,

$$E_o = -\Phi|\bar{\varepsilon}| + U_o\eta. \qquad [3]$$

When electrons interact only weakly $U_o\eta \ll \Phi|\bar{\varepsilon}|$, in which case E_o is a large negative quantity; the corresponding parabola 1 everywhere lies below the straight line in Fig. 4; hence, the metallic phase is stable throughout the entire T range. This is the situation that prevails for alloys with $x \gtrsim 0.60$. These alloys are, however, expected to be poor metals because the bandwidth W of the e_g band is already small to begin with, and because W is further reduced by the factor $\Phi < 1$.

Curve 3 represents the interesting case where the algebraic sum renders E_o considerably less negative. Now a double intersection of the parabola with the straight line occurs. At low temperatures a metallic phase is stable; the parabola lies energetically below the straight line. As T rises there is a point where a transition to the localized, insulating phase takes place. This latter phase remains stable until the second intersection occurs, at which point there is a transition back to the metallic regime, which then prevails up to high temperatures. One therefore encounters reentrant metallic behavior. Such a situation is experimentally observed in the V_2O_3 alloy system (12).

Curve 4 applies when the kinetic and potential energies are nearly in balance but $U\eta < \Phi|\bar{\varepsilon}|$. One sees that over a limited low temperature range the metallic phase is the stable one, but beyond the intersection point the system switches over to the insulating regime. A second intersection is, in principle, possible, but would occur at very elevated temperatures where the compound is no longer stable. This is believed to be the applicable situation for the $NiS_{2-x}Se_x$ system with $0.38 \lesssim x \lesssim 0.60$.

While the present oversimplified model cannot be expected to be correct in detail it provides a crude rationalization of the experimental observation that the low temperature phase of this set of alloys is metallic (though displaying large resistivities) and that with rising T a gap opens up in the density of states. In the experiments this change actually occurs over a narrow temperature range, rather than as sharply as predicted by the present arguments. The discrepancy arises because a number of important factors have been left out of consideration, such as

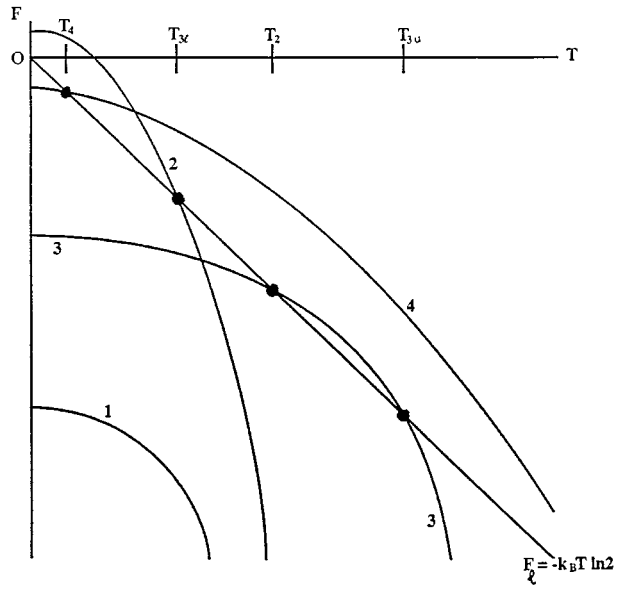

FIG. 4. Proposed qualitative band structure diagram for $NiS_{2-x}Se_x$ alloys. For details see text.

electron–lattice interactions and magnetic ordering phenomena.

Last, curve 2 represents the case where $U\eta$ slightly exceeds $\Phi|\bar{\varepsilon}|$. In this case the intercept E_o is positive; now the insulating phase is stable at low temperatures, and a transition to the metallic state occurs at more elevated T. This is the situation normally encountered in materials exhibiting metal–insulator transformations.

Summarizing, we see that the transitions in Figs. 1b and 1d can be rationalized by assuming that there is a near balance between the kinetic energy of the electrons and the potential energies of their interactions, the latter being somewhat less pronounced. In these circumstances the transition is largely entropy driven.

THERMOELECTRIC PHENOMENA

The Seebeck coefficients (α) of several $NiS_{2-x}Se_x$ alloys are shown in Fig. 2. One of the arresting features of these data is that they do not track the resistivity curves. This violates the general trend whereby materials with high resistivity also display large Seebeck coefficients. In particular, the Seebeck coefficients for NiS_2, or for alloys with low Se content, are very small at cryogenic temperatures, i.e., precisely in the range where the resistivity rises indefinitely as $T \to 0$. Also, in compositions where the alloys exhibit the resistivity humps the Seebeck coefficients remain largely unaffected.

One way of escaping these dilemmas is by invoking the strong correlation effects described earlier: for $x \lesssim 0.35$ the Ni e_g band is split into two subbands as shown in Figs. 3b and 3d. This reflects a more complex band structure wherein the fermi surface in reciprocal space contains several electron and hole pockets. In these circumstances the two subbands are expected to be near mirror images of each other, and the alloys to be almost intrinsic semiconductors. Straightforward analysis (13) shows that the Seebeck coefficients of such intrinsic materials are given by

$$\alpha = -\frac{k_B}{e}\left[\frac{c-1}{c+1}\left(2+\frac{\varepsilon_G}{k_B T}\right)+\frac{3}{4}\ln\frac{m_n}{m_p}\right], \qquad [4]$$

where e is the magnitude of the electronic charge, c is the ratio of electron to hole mobility, ε_G is the relevant gap, and m_n and m_p are the effective masses of electrons and holes, respectively. In the present case it is expected that $c \approx 1$ and that $m_n = m_p$, whence α is almost zero and virtually independent of temperature. This rationalizes the experimental observations for the compositions $x \lesssim 0.35$ at low temperatures. If additionally the gaps Δ and U are comparable, with $\Delta > U$, as in regime d of Fig. 3, then with rising temperature charge carriers will in increasing numbers be promoted from the wide $p\sigma^*$ into the narrow e_g bands. The much more mobile carriers in the $p\sigma^*$ states dominate the electrical characteristics, so that the alloys gradually assume the thermoelectric properties of semiconductors for which hole transport in a single band dominates. α therefore rises with increasing T toward the larger values assumed by this class of materials. This trend is ultimately interrupted by the continually increasing density of mobile carriers, which gradually renders the alloys more metallic and thereby diminishes α. The Seebeck coefficient then passes through a maximum, while the resistivity simply continues to fall with rising temperature.

A similar explanation is expected to hold for material with $0.38 \lesssim x \lesssim 0.60$. As the Se content rises the cation–anion interactions become stronger and the gap Δ is expected to increase (through a greater degree of hybridization) to the point where thermal excitations from the $p\sigma^*$ to the e_g states become negligible. Because of the larger admixture of anionic states by hybridization the e_g band is now also wider, so that regime a in Fig. 3 should prevail; correspondingly, α has the small values appropriate to a half-filled band. As the Mott–Hubbard transition to the insulating state takes effect with rising temperature, the e_g band splits into the two nearly symmetric subbands. The alloys remain intrinsic, so that Eq. [4] is expected to apply; hence, α still remains small. The sharp rise of ρ with T thus is therefore not mirrored in the Seebeck data. Continued excitation of charge carriers across the Hubbard gap U does not fundamentally alter this situation; α remains small over the entire temperature range under study.

Finally, in the metallic regime $x \gtrsim 0.60$ the standard expression for α of a nearly free electron gas is given

by (13)

$$\alpha = -\pi^2 k_B^2 T/3e\mu_0, \qquad [5]$$

where μ_0 is the energy difference between the fermi level and the conduction band edge. The linear T variation and anticipated small values of α are reflected in Fig. 2b, in which the greatly expanded ordinate scale exaggerates even submicrovolt fluctuations of the thermoelectric voltages.

SPECTROSCOPIC STUDIES

There remains one unresolved issue: In a study of ultraviolet photoemission spectroscopy of NiS_2 (14) the researchers stress their belief that the highest occupied state is S 3*p*-like and not Ni 3*d*-like. This would seem to invalidate the prior arguments and speak in favor of regime c of Fig. 3. However, one must recall in these experiments one does not directly observe any transitions but only the Ni 3*d* and S 3*p* densities of state. Furthermore, in ultraviolet spectroscopy the intensity of d–d^* transitions is much lower than the intensity of S 3*p*–Ni 3*d* transitions. Thus, the stronger p–d excitations mask the much weaker spectroscopic d–d transitions. In these circumstances, so long as the $p\sigma^*$ states lie slightly lower in energy than the 3*d* states, the electronic properties at low temperatures are governed by the d–d^* energy separation, whereas truly spectroscopic measurements should reflect the 3*p*–3*d* energy differences.

CONCLUSIONS

On the basis of electrical resistivity and Seebeck coefficient measurement, arguments have been adduced to indicate that the likely qualitative band structure scheme that prevails for $NiS_{2-x}Se_x$ is that shown in Figs. 3a, 3b, and 3d. For alloys with small admixtures of Se scheme Fig. 3b is compatible with the data. As x is increased the Mott–Hubbard and charge transfer excitation gaps become comparable, as shown in Fig. 3d. For alloys with $x \geq 0.65$ the band structure may be characterized by Fig. 3a. However, the great difference in potential of Se^{2-} vs S^{2-} energies, with respect to the hybridization involving Ni $3e_g$ levels, renders likely the onset of Anderson localization states in the wings of the e_g band. This may account for the very poor metallic behavior of alloys with a high Se content, $x \geq 0.65$.

Obviously, these qualitative considerations must ultimately be supplanted by reliable quantitative band structure calculations that follow up the initial efforts cited in Refs. (7–9). These then need to be extended to the more general class of transition metal chalcogenides to characterize the pioneering experimental research in this area by Rouxel and co-workers.

ACKNOWLEDGMENTS

The author is enormously indebted to his collaborators and co-workers who accumulated the experimental data cited in Figs. 1 and 2. He acknowledges many stimulating conversations with Professor J. Spałek concerning electron correlation effects. This research was supported by NSF Grant DMR 96-12130.

REFERENCES

1. R. J. Bouchard, J. L. Gillson, and H. S. Jarrett, *Mater. Res. Bull.* **8,** 489 (1973); H. S. Jarrett, R. J. Bouchard, J. L. Gillson, G. A. Jones, S. M. Marcus, and I. F. Weiher, *Mater. Res. Bull.* **8,** 877 (1973).
2. X. Yao, J. M. Honig, T. Hogan, C. Kannewurf, and J. Spałek, *Phys. Rev. B* **54,** 17469 (1996); X. Yao, S. Ehrlich, G. Liedl, T. Hogan, C. Kannewurf, and J. M. Honig, *Mater. Res. Soc. Proc.* **453,** 291 (1997).
3. X. Yao and J. M. Honig, *Mater. Res. Bull.* **29,** 709 (1994).
4. P. Kwizera, M. S. Dresselhaus, and D. Adler, *Phys. Rev. B* **21,** 2328 (1980).
5. J. B. Goodenough, *J. Solid State Chem.* **3,** 26 (1971); **5,** 144 (1972).
6. J. Rouxel, *Accts. Chem. Res.* **25,** 328 (1992); *Adv. Synth. React. Solids* **2,** 27 (1994), and references therein.
7. S. Lauer, A. X. Tradutwein, and F. E. Harris, *Phys. Rev. B* **29,** 6774 (1984).
8. A. E. Bocquet, T. Mizokawa, T. Saitoh, H. Namatamo, and A. Fujimori, *Phys. Rev. B* **46,** 3771 (1992).
9. A. E. Bocquet, K. Mayima, T. Mizokawa, A. Fujimori, T. Miyadai, H. Takahashi, M. Môri, and S. Suga, *Phys. Condens. Matter* **8,** 2389 (1996).
10. T. Zaanen, G. A. Sawatsky, and J. W. Allen, *Phys. Rev. Lett.* **55,** 418 (1985).
11. J. Spałek, A. Datta, M. Acquarone, and J. M. Honig, *J. Magn. Magn. Mater.* **54–57,** 1335 (1986); J. Spałek, A. Datta, and J. M. Honig, *Phys. Rev. Lett.* **59,** 728 (1987); J. Spałek, A. Kokowski, and J. M. Honig, *Phys. Rev. B* **39,** 4175 (1989); J. Spałek, M. Kokowski, A. Datta, and J. M. Honig, *Solid State Commun.* **70,** 911 (1989).
12. H. Kuwamoto, J. M. Honig, and J. Appel, *Phys. Rev. B* **22,** 2626 (1980).
13. T. C. Harman and J. M. Honig, "Thermoelectric and Thermomagnetic Phenomena and Applications," Chap. 3. McGraw–Hill, New York, 1967.
14. A. Fujimori, K. Mayima, T. Mizokawa, T. Miyadai, T. Sekiguchi, H. Takahashi, N. Môri, and S. Suga, *Phys. Rev. B* **54,** 16329 (1996).